In vitro and In vivo models for studying endothelial cell development and hereditary hemorrhagic telangiectasia

Gkatzis, K.

Chapter 05

"...The effect of TGFβ and BMP9 in endothelial cells is highly dependent on the cellular context..."

Endoglin haploinsufficency in endothelial cells from Rendu- Osler-Weber patient derived induced pluripotent stem cells leads to upregulation of MTUS1 gene expression.

Konstantinos Gkatzis[1], Christian Freund[1], Frank Lebrin[4], Peter ten Dijke[2], Robert Passier[1], Cornelius J.J. Westermann[3], Repke Snijder[3], Hans Jurgen Mager[3],Valeria V. Orlova[1] , Christine L. Mummery[1]*

[1] Leiden University Medical Center, Department of Anatomy and Embryology, Leiden, The Netherlands, [2] Leiden University Medical Center, Department of Molecular Cell Biology, Cancer Genomics Centre Netherlands, Leiden, The Netherlands,[3] St Antonius Hospital, Department of Pulmonary Disease, Nieuwegein, The Netherlands,[4] Center for Interdisciplinary Research in Biology (CIRB), Collège de France, Paris, France*To whom correspondence should be addressed: C.L.Mummery. Leiden University Medical Center, Department of Anatomy and Embryology, Leiden, The Netherlands. Tel: +31-71-5269307. E-mail:c.l.mummery@lumc.nl

Endoglin (ENG), an accessory receptor for selected members of the transforming growth factor β (TGFβ) family, is mainly expressed by endothelial cells (ECs) and mononuclear cells (MNCs) in peripheral blood. Mutations in ENG in humans causes Rendu-Osler-Weber syndrome or Hereditary Hemorrhagic Telangiectasia type 1 (HHT1). Using human induced pluripotent stem cells (hiPSC) generated from HHT1 patients, we derived ECs in which ENG expression was constitutively reduced with view to explore the consequences for ligand induced signaling and EC function. Some features of ECs are affected by cell culture density. We therefore first examined TGFβ downstream Smad activation upon BMP-9 or TGFβ ligand binding as a function of cell density. At low cell densities, ligand stimulation resulted in the expected canonical TGFβ downstream signal activation of intracellular effectors SMAD2 and SMAD1/5 respectively, whereas at high cell density, cross reactivity with other TGFβ family signaling pathways was observed. ENG expression itself was cell density dependent. Consistent with this, we showed that ENG had a prominent role in both canonical BMP9/SMAD1/5 and TGFβ3/SMAD2 phosphorylation under low cell density culture conditions, whereas at high cell densities ENG was only crucial for TGFβ3/SMAD1-5 activation. Global gene expression analysis of HHT1 hiPSC-ECs compared with controls showed a number of differentially expressed genes, most striking of which was microtubule associated tumor suppressor 1 (MTUS1). Upregulation of mRNA and protein in response to siRNA knockdown and examination of vessels in HHT1 patient skin confirmed the inverse relationship between ENG and MTUS1 expression in vitro and in vivo.

Introducion

The discovery that somatic cells in humans can be reprogrammed to a pluripotent state as induced pluripotent stem cells (hiPSC) (Takahashi et al., 2007; Yu et al., 2007) has presented unprecedented opportunities to study cell types normally inaccessible for research as biopsies. These include cells of the cardiovascular system like cardiomyocytes, endothelial cells (ECs), smooth muscle cells and epicardial cells (Cheung et al., 2012; Choi et al., 2009; Witty et al., 2014; Zhang et al., 2009).

Endothelial cells from hiPSC from healthy individuals (hiPSC-ECs) offer opportunities to model early human vascular development (Choi et al., 2009; Rafii et al., 2013), whereas hiPSC-ECs derived from patients with genetic vascular disorders in principle enable research on the molecular alterations responsible for vascular disease pathology (Kinnear et al., 2013). Hereditary hemorrhagic telangiectasia (HHT) or Rendu-Osler-Weber syndrome, is an autosomal dominant vascular disorder, which affects 1:5000 individuals. The major clinical symptoms are arteriovenous malformations (AVMs), ranging from small AVMs or telangiectases in the nasal septum, oral mucosa and gastrointestinal tract to large AVMs in lung, brain and liver. Most cases of HHT are caused by mutations in one of two receptors of the transforming growrh factor (TGF)β family, endoglin (*ENG)* or activin receptor-like kinase 1 (*ALK1* or *ACVRL1)*, which are mainly expressed by ECs and lead to HHT1 and HHT2, respectively (Shovlin, 2010). Haploinsufficiency for ENG or ALK1 has been shown to be the underlying cause of HHT (Pece-Barbara et al., 1999). TGFβ receptors regulate transcription via receptor-dependent phosphorylation of SMAD proteins (Pardali et al., 2010), where their nuclear accumulation mediates downstream transcriptional responses. Previous studies have shown that studying the signaling responses to TGFβ ligands is confounded by effects of culture density in many cell types: signaling appears coupled to cell density (Petridou et al., 2000; Varelas et al., 2010; Zieba et al., 2012) making interpretation of the relevance to endothelial cells *in vivo* and *in vitro* difficult. How endoglin and cell density are coupled and affect TGFβ signaling in healthy hiPSC-ECs and HHT1 hiPSC-ECs is unknown. Since we wished to use hiPSC-EC as a model for studying HHT1 to investigate the consequences of reduced ENG in ECs, a necessary prelude was to determine ligand responses as a function of EC culture density. We found that cell density is an important determinant for SMAD activation in hiPSC-ECs and that ENG haploinsufficiency in response to TGFβ family members. Under controlled cell density culture conditions we were then able to compare hiPSC-ECs from healthy controls and from an HHT1 individual by microarray; this showed that *ENG* was reduced as expected but another gene (*MTUS1*), which has been previously linked to TGFβ signaling in chicken (Kosla et al., 2013), was strikingly upregulated. Delivery of two different ENG siRNAs in control hiPSC-ECs resulted in the upregulation of MTUS1 mRNA and protein levels, further suggesting the direct link between ENG and MTUS1. This was shown at the protein and mRNA level to be independent of cell density by siRNA knockdown in control hiPSC-EC. Further, MTUS1 was upregulated *in vivo* in human skin ECs from HHT1 patients. Thus *MTUS1* is a new TGFβ signaling candidate gene that is highly upregulated when ENG levels are reduced.

Results

ENG and cell proliferation of hiPSC-derived EC cells

Several studies in mouse and human tissues have indicated that endoglin is broadly expressed in endothelium during development as vessels form through angiogenesis but that it is expressed at low levels in quiescent adult endothelium (Lebrin et al., 2004). However, it is upregulated when endothelium is activated, for example as an injury response following tissue damage or during inflammation (van Laake et al., 2006). Whether this is cause or effect

is unknown. Here, we exploited some recently generated hiPSC lines from HHT1 patients (Orlova et al in prep;(Freund et al., 2010)) to determine whether ECs from these HHT1 hiPSC lines showed reduced proliferation *in vitro.*

We first measured the levels of ENG mRNA and protein in hiPSC-ECs to determine whether these had been maintained at the (reduced) levels in mononuclear cells in peripheral blood from HHT1 patients (Orlova et al, in prep) during the reprogramming process. hiPSC-ECs were derived as described previously (Orlova et al., 2013; 2014) from control and ENG mutant hiPSC lines. Constitutively reduced ENG mRNA and protein levels were detected in HHT1 patient hiPSC-ECs when compared to controls **(Fig.1A, Fig.1B**). Proliferation was then assessed as the number of human ECs after 24, 36, 48, 60 and 84 hours of plating in culture in the presence of low concentrations of VEGF. Growth rates were similar over the whole time course (**Fig.1C**) suggesting that reduced ENG within this range does not affect proliferation of these patient derived hiPSC-derived ECs in culture.

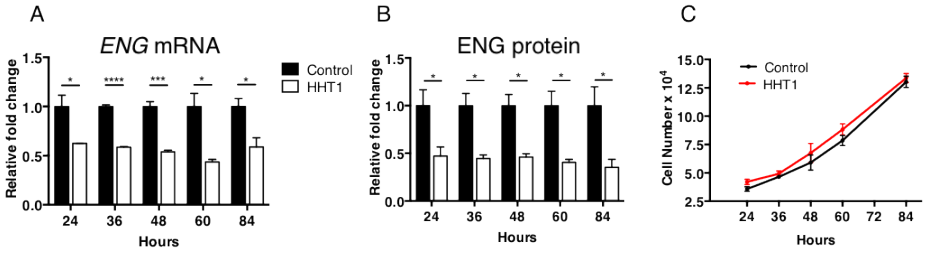

Figure 1. Reduced levels of ENG in HHT1 iPSC-ECs (HHT1) are not affected in cell proliferation. hiPSC-ECs were grown for 24, 36, 48, 60 and 84 hours in culture, when *ENG* mRNA, protein levels and cell number were measured. **A.** *ENG* mRNA levels in Control and HHT1 hiPSC-ECs measured by RT-qPCR (*n*=3). **B.** ENG protein levels in Control and HHT1 hiPSC-ECs measured by FACs (n=3). **C.** Proliferation growth rates assessed as the cell number of Control and HHT1 hiPSC-ECs (*n*=3). All error bars represent s.e.m. **P* < 0.05, ***P*< 0.01, ****P* <0.001, and *****P* <0.0001, results from unpaired t test.

Cell density affects TGFβ signalling in hiPSC-ECs.

In most cell types TGFβ binding to its cell surface receptors induces phosphorylation of SMAD2 via ALK5 but exceptionally in ECs, TGFβ phosphorylates ALK1. ALK1 in turn recruits and phosphorylates SMAD1/5, normally activated by BMP signaling (Pardali et al., 2010). Furthermore, previous studies have demonstrated that SMAD protein variations in response to TGFβ can be cell density-depended (Petridou et al., 2000; Zieba et al., 2012). For biologically meaningful comparisons of the properties of different types of ECs it is therefore essential that cells are harvested or analyzed at the same cell density. Since ENG is a co-receptor in the signaling complex, we examined how cell density affected phosphorylation of SMADs prior to comparing control hiPSC-ECs and HHT1 hiPSC-ECs.

We first investigated which ligands were able to phosphorylate SMAD1/5 or SMAD2 proteins selectively in control hiPSC-ECs under subconfluent culture conditions using Western blot analysis. BMP-9 and TGFβ-3 activated (phosphorylated) SMAD1/5 and SMAD2 proteins, respectively, with a peak response 30-60 min after first exposure (**Supplementary Fig.1A**). Since BMP and TGFβ can cross-react with each other's receptors at high concentrations (Brown et al., 2005; Suzuki et al., 2010; Thomas et al., 2007), we determined the effects of low (0.1ng/ml) and high (2ng/ml) concentrations of each ligand as a function of cell density (**Supplementary Fig.1B**). Density categories were based on cell number per unit of surface

area of the culture dish (35-50x10^3 (low) and 1.25-1.50 x10^5 (high) cells, respectively). SMAD1/5/8 and SMAD2 were stimulated in control hiPSC-ECs by BMP-9 and TGFβ-3, respectively, at both low and high cell densities. Of note, cell density alone affected ENG protein levels: these were significantly lower at high cell densities compared with low (**Supplementary Fig.2A**).

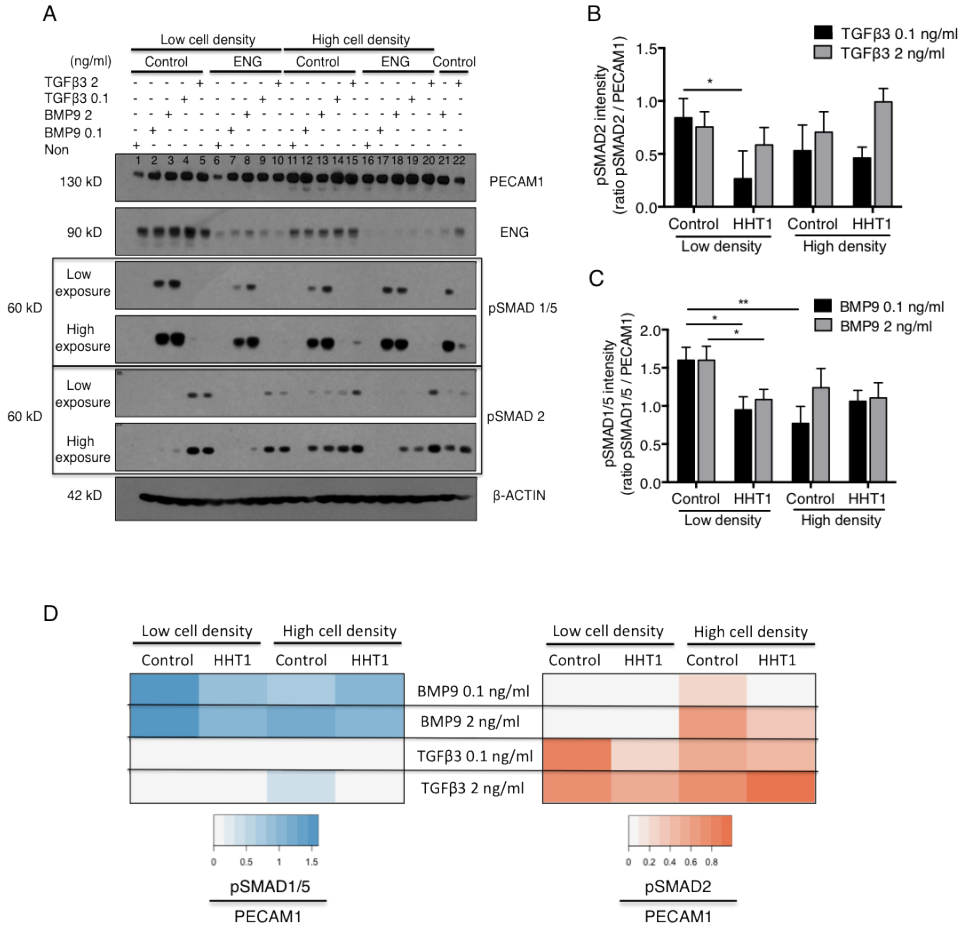

Figure 2. Cell density and reduced levels of ENG affect activation of downstrem TGFβ SMAD proteins. hiPSC-ECs were stimulated with low or high concentrations of BMP9 and TGFβ3 ligands under low or high cell density culture conditions and downstream phosphorylation of SMAD proteins was assessed. A. Western blot analysis of stimulated hiPSC-ECs. High exposure times were used for the quantification in B and C. B. Histogram showing quantification of SMAD1/5 phosphorylation relative to PECAM1 in control and HHT1 hiPSC-ECs cultured in low and high cell density (n=3). C. Quantification of SMAD2 phosphorylation in stimulated control and HHT1 hiPSC-ECs cultured under low or high cell density conditions (n=3). D. Heatmap showing pSMAD intensity of Figure2A. The data are presented as ratio of pSMADs / PECAM1(n=3). All error bars represent s.e.m. *$P < 0.05$, **$P < 0.01$, results from unpaired t test.

TGFβ-3 stimulation at both low and high concentrations phosphorylated SMAD2 proteins in control hiPSC-ECs equally at both high and low cell densities, thus was independent of cell density (**Fig.2A** Lane 4-5 versus14-15, **Fig.2A**). High concentrations of TGFβ-3 however

also phosphorylated Smad1/5 proteins although only at high cell densities (**Fig.2A** Lane 5 versus15). This indicated that cross-phosphorylation of SMAD1/5 by TGFβ-3 in hiPSC-ECs was dependent on cell culture density.

Investigation of the effects of BMP-9 ligand on control hiPSC-ECs by contrast showed different density dependencies of SMAD activation. More specifically, at both high and low cell densities, BMP9 induced SMAD1/5 phosphorylation in a concentration dependent manner but at low cell density the absolute levels of pSMAD1/5 were higher than at high cell density (**Fig.2A** Lane 2 versus12, **Fig.2B**). Furthermore, both low and high concentrations of BMP-9 significantly phosphorylated SMAD2 protein but only under high cell density culture conditions (**Fig.2A** Lane 2-3 versus12-13). These results indicated that phosphorylation of SMAD1/5 and SMAD2 upon BMP-9 stimulation is ligand concentration and cell density dependent

Cell density affects gene expression levels of TGFβ related genes

To investigate whether the pattern of phosphorylated SMADs at different cell densities was caused by differences in expression levels of components of the signaling pathway, we examined the expression of genes encoding the TGFβ family of receptors.

Control hiPSC-ECs were cultured and collected from low and high cell density cultures; mRNA expression was determined using RT-qPCR. *ENG* mRNA was significantly lower at high cell densities compared to low, confirming the Western blot data at the protein level (**Fig.3A**, **Supplementary Fig.2A**). Some, but not all, of other TGFβ receptor family genes were also affected by cell density. For example, *ALK5*, *ALK2* and *TGFβRII* mRNA levels decreased at high cell densities compared to low (**Fig.3B, 3C and 3F**), whereas *ALK1* and *BMPRII* levels were not altered (**Fig.3D and 3E**). These findings indicated that cell density can affect expression of genes associated with TGFβ signaling so that care should indeed be taken to analyse hiPSC-ECs from different (ENG mutant) lines at the same density.

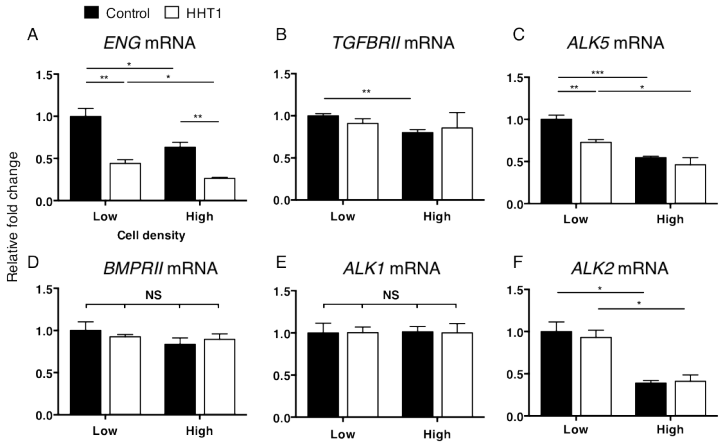

Figure 3. Endothelial cell density and reduced levels of ENG affect the gene expression of certain TGFβ related receptors. We measured mRNA levels of TGFβ related receptors in control and HHT1 hiPSC-ECs after grouping them into low (35-50 x 103 cells) and high (125-150 x 103 cells) cell densities. Values were additionally normalized to endothelial specific marker, PECAM1. A. *ENG* B. *TGFBRII* C. *ALK5* D. *BMPRII* E. *ALK1* and F. *ALK2* mRNA levels in Control and HHT1 hiPSC-ECs cultured under low and high cell densities (n=3). All error bars represent s.e.m. *$P < 0.05$, **$P < 0.01$ and ***$P < 0.001$, results from unpaired t test. NS, not significant.

Reduced ENG in HHT1 hiPSC-ECs affects TGFβ signaling only at low cell density.

As indicated above, ECs are sensitive to density in culture: their response to BMP-9 and TGFβ -3 ligands and gene expression associated with TGFβ signaling all change in the transition from low- to high density. Since ENG is a co-receptor in the TGFβ signaling complex and its protein levels are cell density dependent, we examined its effect on SMAD phosphorylation at low and high cell density. We stimulated HHT1 hiPSC-ECs with low (0.1 ng/ml) and high (2 ng/ml) concentrations of BMP-9 and TGFβ-3 ligands at both low and high cell densities and compared phosphorylation of SMAD1/5 and SMAD2 proteins with control hiPSC-ECs.

We first focused on low cell density and the phosphorylation of SMAD1/5 and SMAD2 proteins upon stimulation with BMP-9 and TGFβ-3, respectively.
Stimulation with either low or high concentrations of BMP-9 revealed significantly reduced levels of pSMAD1/5 in HHT1 hiPSC-ECs compared with controls (**Fig.2A** Lane 2-3 versus 7-8, **Fig.2C**). This indicated the importance of ENG for pSMAD1/5 stimulation by BMP-9. Notably, HHT1 hiPSC-ECs also exhibited significantly lower levels of pSMAD2 compared to controls but when stimulated only with low concentrations of TGFβ-3 (**Fig.2A** Lane 4 versus 9, **Fig.2B**, **Fig.2D**). These results indicated the importance of ENG for phosphorylation of SMAD2 protein upon stimulation with low concentrations of TGFβ-3 under low cell density culture conditions.

We next examined pSMAD1/5 and pSMAD2/3 protein under high cell density conditions. BMP-9 stimulation showed activation of SMAD1/5 proteins (**Fig.2A** Lane 12-13 versus 17-18, **Fig.2C**) and SMAD2 proteins (**Fig.2A** Lane 12-13 versus17-18, **Fig.2D**) but without significant consistent differences between control and HHT1 hiPSC-ECs. This confirmed that high concentrations of BMP-9 phosphorylate SMAD2 protein and that ENG probably does not have significant role in this process.

TGFβ-3 stimulation at either low or high concentrations resulted in similar levels of pSMAD2 between control and HHT1 hiPSC- ECs (**Fig.2A** Lane 14-15 versus 19-20, **Fig.2B**). Interestingly, stimulation with high concentrations of TGFβ-3 resulted in lower levels of pSMAD1/5 in HHT1 hiPSC-ECs (**Fig.2A** Lane 15 versus 20, **Fig.2D**). The results overall showed that high concentrations of TGFβ-3 can phosphorylate SMAD1/5 proteins and that ENG plays a key role in this process.

Reduced ENG in HHT1 hiPSC-ECs alters TGFβ superfamily receptor expression in a cell density dependent manner

Reduced levels of endoglin in MEECs derived from mutant mouse embryos or after knock-down experiments have been reported to either upregulate or downregulate *alk5* expression (Lebrin et al., 2004; pece-Barbara et al., 2005). In order to understand the differences in SMAD phosphorylation between control and HHT1 hiPSC-ECs and find out whether reduced ENG in HHT1 hiPSC-ECs affects *ALK5* expression or other TGFβ family receptors, we determined their expression by RT-qPCR at high and low densities. As expected from Western blotting, HHT1 hiPSC-ECs had significantly lower levels of *ENG* mRNA at both cell densities compared with controls hiPSC-ECs (**Fig.3A**). We next analyzed the expression of *ALK1*, *ALK2*, *ALK5*, *TGFβRII* and *BMPRII*. In accordance with the result in endoglin mutant mouse ECs, *ALK5* expression was also significantly reduced at low cell densities (**Fig.3C**). *ALK1*, *ALK2* and *BMPRII* expression was unaffected by reduced levels of ENG (**Fig.3D, 3E, 3F**) independent of cell density.

Thus endogenous reduction of ENG can reduce the expression of important signaling receptors of TGFβ in hiPSC-ECs, which may in turn affect their response to ligands but this effect is cell density dependent in culture.

Reduced levels of ENG lead to the upregulation of MTUS1, a microtubule associated tumor suppressor

Previous gene expression analysis of human umbilical vein endothelial cells (HUVEC) from newborns with ENG mutations revealed multiple differentially expressed genes when compared to healthy control cells (Thomas et al., 2007). The major caveat of this study however was that clinical signs of HHT1 are not evident in HUVECs because of their high levels of ENG when cultured (Chan et al., 2004; Ota et al., 2002). In order to overcome this issue of extraordinarily high levels of ENG, we analysed global gene expression in control and HHT1 hiPSC-ECs derived from genetically confirmed HHT1 patient with severe disease symptoms. In light of the observed effects of hiPSC-EC density of TGFβ pathway signaling components, we harvested the cells from cultures at high cell density.

Microarray analysis showed 41 differentially expressed genes between control and HHT1 hiPSC-ECs (**Fig.4A**). As expected from the qPCR data above, *ENG* mRNA levels were significantly reduced in HHT1 ECs. One of the genes that was highly upregulated in HHT1 hiPSC-ECs and that has not been previously characterized in human ECs but its expression has been correlated with the early angiogenic pattern of ENG, was microtubule associated tumor suppressor 1 (*MTUS1*) (Bundschu and Schuh, 2014). Upregulation of *MTUS1* in HHT1 hiPSC-ECs was further demonstrated by qPCR (**Fig.4B**). To confirm that *MTUS1* upregulation was due to reduced levels of ENG and not to any differences in the cell density, we showed by siRNA-mediated downregulation of *ENG* expression in control hiPSC-ECs that indeed *MTUS1* increased as function of ENG downregulation (**Fig.4C and Supplementary Fig.4A**). We also observed increased levels of *MTUS1* in independently derived HHT1 hiPSC-ECs compared with controls (Supplementary **Fig.4B**). Notably, *MTUS1* mRNA levels were also upregulated in HHT1 hiPSC-ECs at low and high cell densities (**Supplementary Fig.4C**). In addition, MTUS1 protein levels were also upregulated by Western blot analysis when ENG was knocked-down in control hiPSC-ECs (**Fig.4D**).

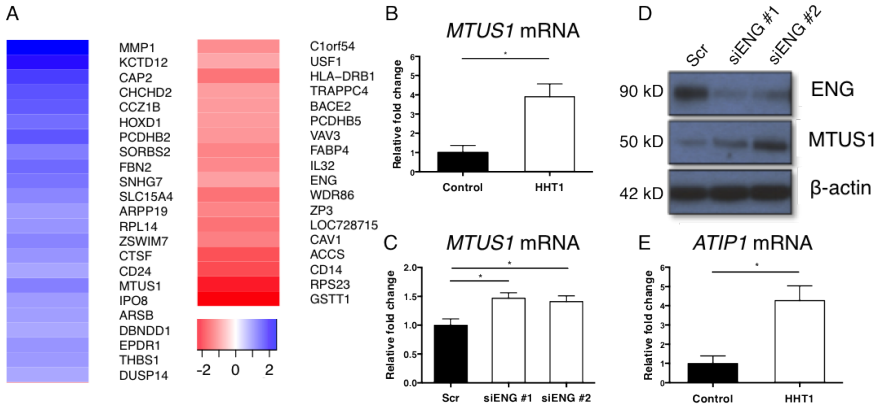

Figure 4. Increased *MTUS1* mRNA and protein levels in iPSC-ECs with reduced levels of ENG. A. Differentially expressed genes identified by microarray analysis. Data are presented as fold change > 2. B. *MTUS1* mRNA levels in Control and HHT1 hiPSC-ECs measured by qPCR (n=3). C and D. *MTUS1* mRNA and protein levels in Control hiPSC-ECs treated with scrambled (control) or two independent ENG-targeting small interfering RNAs (siENG #1, siENG #2)(n=3). E. *ATIP1* mRNA levels in Control and HHT1 hiPSC-ECs (n=3). All error bars represent s.e.m. *$P < 0.05$, results from unpaired t test.

MTUS1 encodes a number of isoforms, termed AT2 receptor-interacting proteins (ATIPs), in humans and nothing is yet known specifically about its role in ECs. We therefore determined which *MTUS1* isoforms are expressed in hiPSC-ECs. We first designed and tested the qPCR primers in human embryonic brain and placenta, organs that have been previously reported to express the different *MTUS1* isoforms (**Supplementary Fig.4D and 4E**) (Di Benedetto et al., 2006). Finally, we found that *ATIP1* is the principle isoform expressed by hiPSC-ECs and that *MTUS1* upregulation in HHT1 hiPSC-ECs is mainly due to upregulation of *ATIP1* (**Fig.4E**).

Increased MTUS1 protein levels in HHT1 skin biopsies

The *in vitro* findings that MTUS1 expression is increased in HHT1 hPSC-ECs led us to the test whether MTUS1 is also upregulated *in vivo*. We first examined the expression of ENG in sections of human nasal mucosal biopsies from HHT1 patients compared to a healthy individual and found that ENG protein levels were significantly reduced (**Fig.5A**). We then examined the expression of MTUS1 in the same specimens to see whether there was an inverse correlation between ENG and MTUS1 protein levels *in vivo*. We confirmed this relationship by showing substantially higher MTUS1 staining in the endothelial layer of HHT1 skin compared to healthy individual (**Fig.5B**).

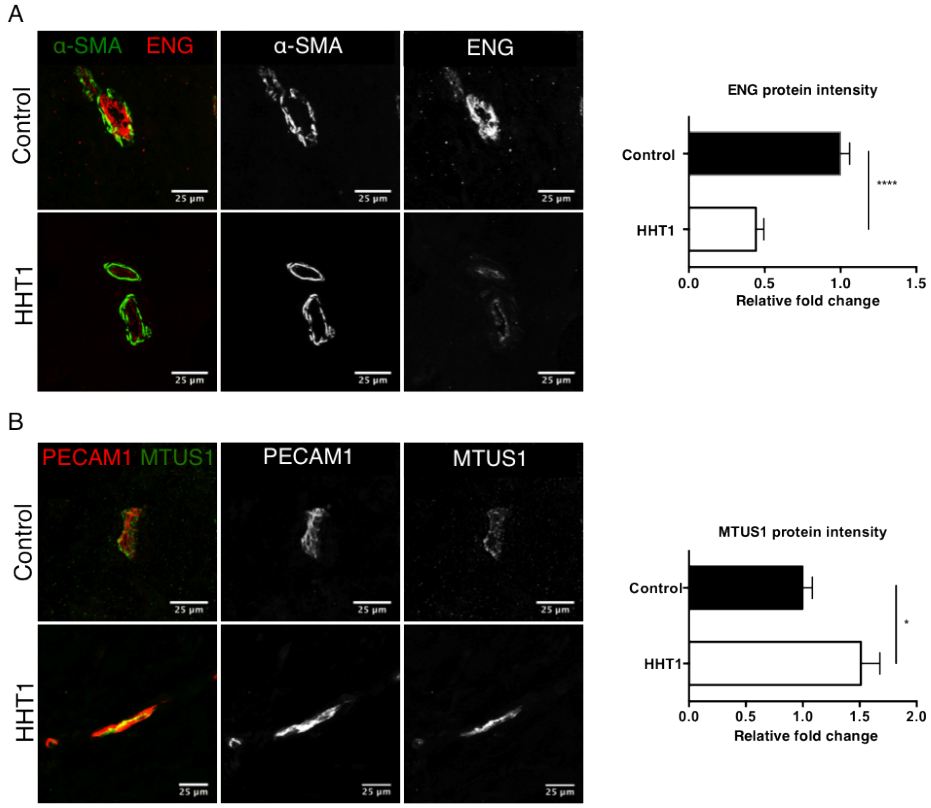

Figure 5. HHT1 human skin exhibits increased MTUS1 protein levels. Confocal images of human skin biopsies from Control and HHT1 individuals. A. Left, α-smooth muscle actin (α-SMA) in green and ENG immunostaining in red. Right, quantification of ENG staining intensity (n= 8) B. Left, PECAM1 (red) and MTUS1(green) immunostaining. Right, quantification of MTUS1 staining intensity normalized to PECAM1 intensity (n= 8). All error bars represents.e.m. *P < 0.05 and ****P <0.0001, results from unpaired t test.

Discussion

It has been more than 20 years since the cloning of endoglin (Gougos and Letarte, 1990) and since then its functional role in TGFβ signaling has been extensively characterized. *In vitro* studies using various EC lines have clearly demonstrated that endoglin is crucial for downstream "canonical" and "cross-over" TGFβ signaling pathway activation. Here, we demonstrated that ECs derived from control- or HHT1 hiPSC lines can be used to reveal downstream TGFβ signaling differences and that cell culture density is an important factor in determining signaling responses and thus their interpretation.

We chose to use control and HHT1 iPSC-ECs because they serve as healthy- and diseased human EC models respectively and can be used to study human physiological and pathological cell responses. Since hiPSC-ECs have only been used recently to study downstream TGFβ signaling (Orlova et al, in prep), we first identified BMP-9 and TGFβ-3 as the most reliable cytokines for "canonical" (BMP-9/SMAD1/5 and TGFβ-3/SMAD2) SMAD activation. As observed in mouse embryonic ECs (MEEC) and bovine aortic endothelial cells (BAEC) (Goumans et al., 2003), high concentrations of TGFβ-3 induced phosphorylation not only of SMAD2 but also of SMAD1/5 in control hiPSC-EC but only at high cell density. In line with this, by comparing the control hiPSC-ECs and those from HHT1-ECs, we could confirm that, as described by others, (Blanco et al., 2005; David et al., 2007; Lebrin et al., 2004), ENG is required for TGFβ-3/ALK1-mediated activation of SMAD1/5 in hiPSC-ECs. This was further supported by our finding that ENG mRNA and protein were reduced in hPSC-ECs at high cell densities. Additionally, only at high cell densities, were we able to detect phosphorylation of SMAD1/5 and SMAD2 upon stimulation with BMP-9. This finding is consistent with a study using human pulmonary artery endothelial cells (PAECs), in which phosphorylation of SMAD1/5 and SMAD2 via BMPRII/ActRII/ALK1 was induced by BMP-9 stimulation (Upton et al., 2009).

At low cell densities, we did not detect any "cross-over" in TGFβ induced SMAD phosphorylation, which highlights the importance of studying EC responses in precisely defined ranges of cell density, rather than unknown conditions under which signaling "cross-over" may or may not occur. Although there was no "cross-over" at low cell density, it appears that ENG is able to potentiate BMP9/ALK1/pSMAD1/5 signaling. Indeed, in NIH-3T3 fibroblasts, endoglin overexpression only increased BMP9-induced BRE promoter activity and not that by BMP-2 (David et al., 2007; Nolan-Stevaux et al., 2012). As observed in endoglin-depleted MEECs (Lebrin et al., 2004), reduced *ALK5* mRNA expression was also detected in HHT1 hiPSC-ECs under low cell densities. This finding, in combination with the reduced phosphorylation of SMAD2, suggested that ENG and ALK5 are required for "canonical" TGFβ-3/ALK5/pSMAD2 signaling. The latter is also confirmed by more recent evidence using HUVECs (Nolan-Stevaux et al., 2012).

We then sought to elucidate whether under defined conditions we could identify genes affected by reduced levels of ENG. Microarray analysis of HHT1 hiPSC-ECS revealed alterations in the expression levels of 41 genes, among which MTUS1 had not been described before in ECs. We confirmed the direct dependence of MTUS1 on ENG levels by siRNA knockdown of ENG and showed that both mRNA and protein were upregulated by reduced ENG in hiPSC-ECs. Our data also provide the first evidence of *ATIP-1* as the predominant isoform of *MTUS1* in both control and HHT1 hiPSC-ECs although further investigation will be required to reveal its function in these cells. MTUS1 protein is expressed in the developing mouse cardiovascular system, including vascular plexus of the yolk sac and is strongly correlated with the early angiogenic pattern of endoglin(Bundschu and Schuh, 2014). Additionally, MTUS1 has been identified as upregulated upon inhibition of TGFβ signaling in chicken

embryo dermal myofibroblasts (Kosla et al., 2013), thereby further suggesting its association with TGFβ signaling. Nevertheless, our demonstration of a marked MTUS1 increase in HHT1 patient skin corroborates its association with endoglin and further suggests a possible role in the pathogenesis of HHT, which remains to be fully elucidated.

Methods

Generation of human induced Pluripotent Stem Cells (hiPSCs)
Control iPSC and HHT1 patient-specific (HHT1, exon 5 IVS 5+2 (T>C)) iPSC were generated and characterized previously ((Freund et al., 2009); Orlova et al. in prep). Briefly, fibroblast from skin biopsies and blood outgrowth endothelial cells (BOECs) from peripheral blood were used along with a self-inactivating polycistronic lentivirus system for reprogramming(Dambrot et al., 2013).

hiPSC culture and endothelial cell differentiation
hiPSC were maintained and differentiated to endothelial cells as previously described (Orlova et al., 2013). Briefly, hiPSC lines were grown in serum-free, mTeSR1 (Stem Cell Technologies) medium and penicillin-streptomycin (5,000 U ml^{-1}, Gibco). They were enzymatically passaged once a week on Matrigel (BD Biosciences) -coated 6-well plates. hiPSC were differentiated in monolayer culture using sequential treatment of growth factor addition, as follows: VEGF (50ng/ml, R&D Systems), BMP4 (30ng/ml, Miltenyi Biotec), Activin A (25ng/ml, Miltenyi Biotec), GSK inhibitor CHIR-99021 (1.5uM, Tocris Bioscience) is added for three days to induce mesoderm which is then specified to endothelial cells by SB431542 (10mM, Tocris Bioscience) and VEGF (50ng/ml) for 7 days. Endothelial cells were isolated using CD31-Dynabeads (Invitrogen) and DynaMag-15 magnet (Life Technologies) and plated on gelatin-(Sigma-Aldrich) -coated T75 tissue culture flask with EC culture medium (human endothelial-SFM, Gibco) containing 1% platelet poor plasma derived serum (Biomedical Technologies) and 50ng/ml VEGF until they reach confluence.

EC proliferation assay and cell density categorization
hiPSC-ECs were plated in 24-well plates at a density of 30,000 cells per well. EC culture medium containing 1% platelet poor plasma derived serum and 25ng/ml VEGF was refreshed every 12 hours. Cell proliferation was analyzed by counting the cell number after 24, 36, 48, 60 and 84 hours. Each experiment was performed in triplicate and repeated minimally three times. For low- and high-density cell cultures, 25000 cells were plated in 24-well dishes and grown for 36-48 (35-50x10^3 cells) or 84 hr (125-150 x10^3 cells), respectively.

EC stimulation
hiPSC-EC were seeded in 24-well plates and grown to low or high cell densities as described above. Cells were washed with phosphate-buffered saline (PBS, Gibco) and serum-starved for 5 hours. Cells were stimulated for 30 minutes with 0, 0.1, or 2 ng/ml of BMP9 (R&D Systems) or TGFβ-3 (Peprotech), put on ice, washed with cold PBS and processed for protein extraction.

Flow cytometry
Fluorescence-activated cell sorting (FACs) analysis was performed as described before(Orlova et al., 2013).

Immunohistochemistry of human skin biopsies and quantification
HHT1 and control donor skin samples were obtained from St Antonius Hospital (Department of Pulmonary Disease, Nieuwegein, The Netherlands) and Leiden University Medical Center

(Department of Molecular Cell Biology, Leiden, The Netherlands) respectively. Sections were handled as described previously (Lebrin et al., 2010). Briefly, cryosections (5µm) of HHT1 and control donor skin biopsies were fixed in 2% paraformaldehyde, permeabilized in PBS with 0.1% Triton X100 (Sigma-Aldrich) and blocked in PBS with 4% normal swine serum. Cryosections were incubated with primary or secondary antibodies in blocking solution (4% normal swine serum) overnight at 4C or 2 hours at room temperature, respectively. Primary antibodies: mouse anti-PECAM (1:30, Dako), anti-SMA conjugated to Cy2 (1:200, Sigma-Aldrich), mouse anti-Endoglin (1:100, BD Bioscience), rabbit anti-MTUS1 (1:100, Novusbio). Secondary antibodies: anti-mouse Alexa555 (1:200, Life Technologies) and anti-rabbit Alexa488 (1:200, Life Technologies). Stained cryosections were examined using Confocal Leica-SP5 MP. Eight images for each group and set of immunostainings were taken at the same laser intensity. Anti-SMA, anti-Endoglin, anti-PECAM1 and anti-MTUS1 staining intensity was quantified using Fiji software. For each image the vessels were delineated, in which staining intensity was calculated using the mean grey value function.

Protein extraction, Western blot analysis and Densitometry

Cell lysates were prepared with RIPA buffer (50mM Tris-HCl, 250mM NaCl, 2% NonidentP40, 2.5mM EDTA-Na, 0.1% SDS, 0.5% DOC, pH 7.2) containing complete protease inhibitor cocktail II (Roche Applied Science). Protein concentrations were determined using the DC Protein Assay Kit II (BioRad). Samples were analyzed by Western blot using 10% polyacrylamide gels, followed by overnight wet-transfer of the proteins to activated nitrocellulose membranes Hybond-C Extra (Amersham, Biosciences). Membranes were blocked in TBS-T (0.01 M Tris-HCl, pH 7.4, 0.15M NaCl, 0.1% Tween-20) with 5% dried milk and incubated overnight with the indicated antibodies. Signal detection was performed using the ECL system and SuperSignal West Pico Chemiluminecent Substrate (Thermo Scientific). Signals were quantitatively analysed using ImageJ software. The antibodies used in the study are the following: Goat Endoglin/CD105 (1:1000, R&D Systems), rabbit anti-PECAM1 (1:500, Santa Cruz), mouse anti-β-actin (1:5000, Sigma-Aldrich), rabbit anti-MTUS1 (1:2000, Novusbio), rabbit anti-pSmad1/5 (1:500, Cell Signaling), rabbit anti-pSmad2/3 (1:500, Cell Signaling), HRP-conjugated secondary antibodies anti-rabbit IgG (1:5000, Cell Signaling), HRP anti-goat IgG (1:5000, Santa Cruz), HRP anti-mouse IgG (1:5000, Cell Signaling).

ENG knock down

All transfections were carried out at a final concentration of 5nM in 24-well plates using Oligofectamine (Invitrogen) according to the manufacturer's instructions. Control hiPSC-EC were transfected with two siRNAs directed against human ENG and a non-targeting control siRNA (FlexiTube siRNA, QIAGEN, SI02663024 and SI02663031), si-CONTROL non-targeting siRNA(AllStars Negative Control, QIAGEN, 111754271). The medium was changed after overnight incubation and 48hr after transfection the cells were analysed as indicated.

RNA isolation and Quantitative PCR

Total RNA was isolated using NucleoSpinII RNA Kit (Macherey-Nagel), DNase treated using Ambion TURBO (Life Technologies) and complementary DNA (cDNA) was made from equal amount for all samples using iScriptII (BioRad). Quantitative PCR (CFX96 Real-Time System, Bio-Rad) was performed using oligonucleotide primers for human *ALK1*, *ALK2*, *ALK5*, *ENG*, *BMPRII*, *TGFβRII*, *MTUS1*, *ATIP1*, *ATIP2*, *ATIP4* and the human reference gene *ARP* for normalization. Quantitative PCR was performed using SYBR Green Supermix (Bio-Rad) mixture with an initial denaturation step of 3 min at 95°C followed by 40 cycles of 15 s denaturation at 95°C, 30 s annealing at 60°C, and 45 s extension at 72°C. Technical and

biological replicates were carried out for all quantitative PCR reactions.

Statistical analysis
Experimental data were statistically analyzed with Prism6 software and unpaired/paired Student's *t* test. P values <0.05 were considered statistically significant.

Acknowledgements
We are grateful to C. Oud (Dept. Molecular Cell Biology) for providing the control human skin sample, F. van Hil (Dept. Anatomy and Embryology) for help with cell culture. The work described was supported by grants from SWORO (Stichting Weber-Osler-Rendu, the Netherlands), T. Peek and The Netherlands Heart Foundation (NHS 2008B106).

Supplementary Figures

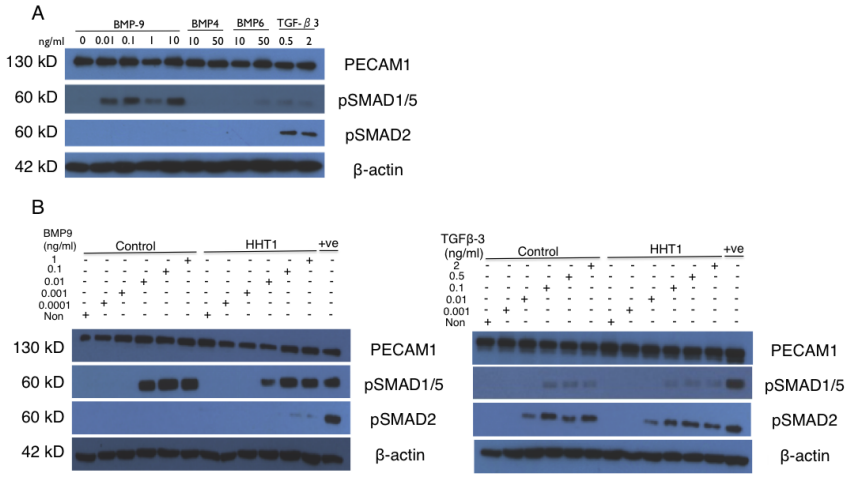

Supplementary Figure 1. Activation of BMP/TGFβ downstream SMAD proteins. hiPSCECs were serum-starved and stimulated under subconfluent cell culture conditions. Downstream phosphorylation of SMAD1/5 and SMAD2 proteins was assessed by Western blot. **A.** Stimulation of Contol hiPSC-ECs with BMP4, BMP6, BMP9 and TGFβ3 ligands for 1 h. **B.** Dose-response of BMP9 and TGFβ3-induced phosphorylation in Control and HHT1 hiPSC-ECs for 1 h. Control hiPSC-Ecs were stimulated either with BMP9 (2ng/ml) or TGFβ3 (2ng/ml) and used as positive controls for pSMA1/5 and pSMAD2 activation, respectively.

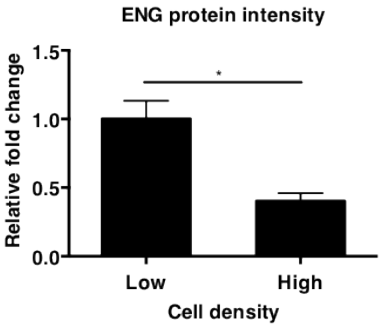

Supplementary Figure 2. ENG protein levels in control hiPSC-ECs. **A.** Histogram showing quantification of ENG protein levels relative to PECAM1 as assessed by Western blot (*n*= 3). All error bars represent s.e.m. **P* < 0.05, results from unpaired t test.

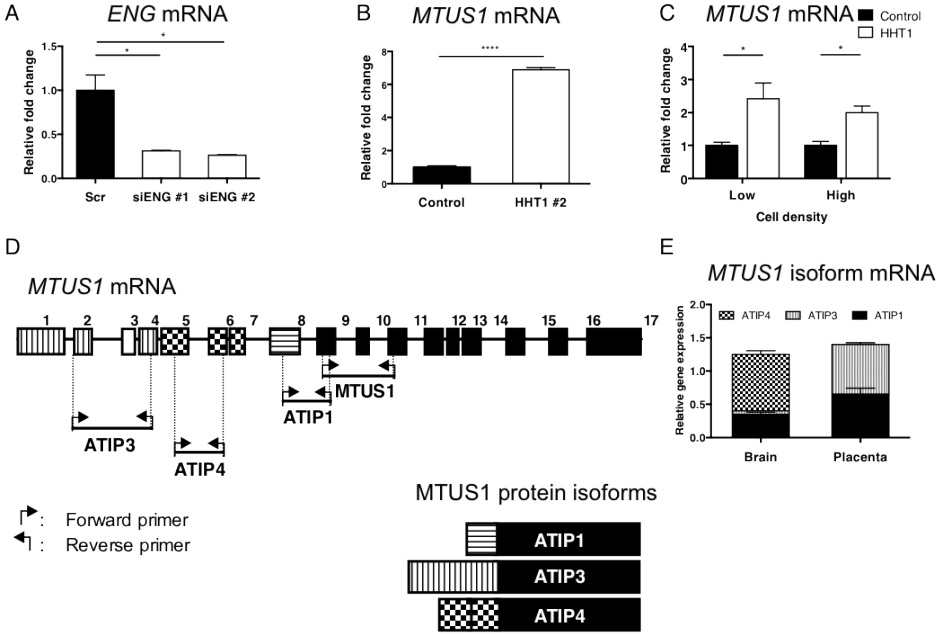

Suplementary Figure 3. Increased *MTUS1* mRNA levels in iPSC-derived ECs with reduced levels of ENG. **A.** *ENG* mRNA levels in Control hiPSC-ECs transfected with Scroble or two different ENG siRNA constructs (n=3). **B.** *MTUS1* mRNA levels in Control and additional HHT1 hiPSC-ECs derived from HHT1 patient with different mutation (*n*=3). **C.** *MTUS1* mRNA levels in Control and HHT1 hiPSC-ECs under low and high cell density conditions (*n*=3). **D.** Schematic representation of *MTUS1* locus with the primers designed to amplify its different isoform (*ATIP1*, *ATIP3* and *ATIP4*). **E.** *ATIP1*, *ATIP3* and *ATIP4* mRNA levels in human embryonic tissue. All error bars represent s.e.m. **P* < 0.05, results from unpaired t test.

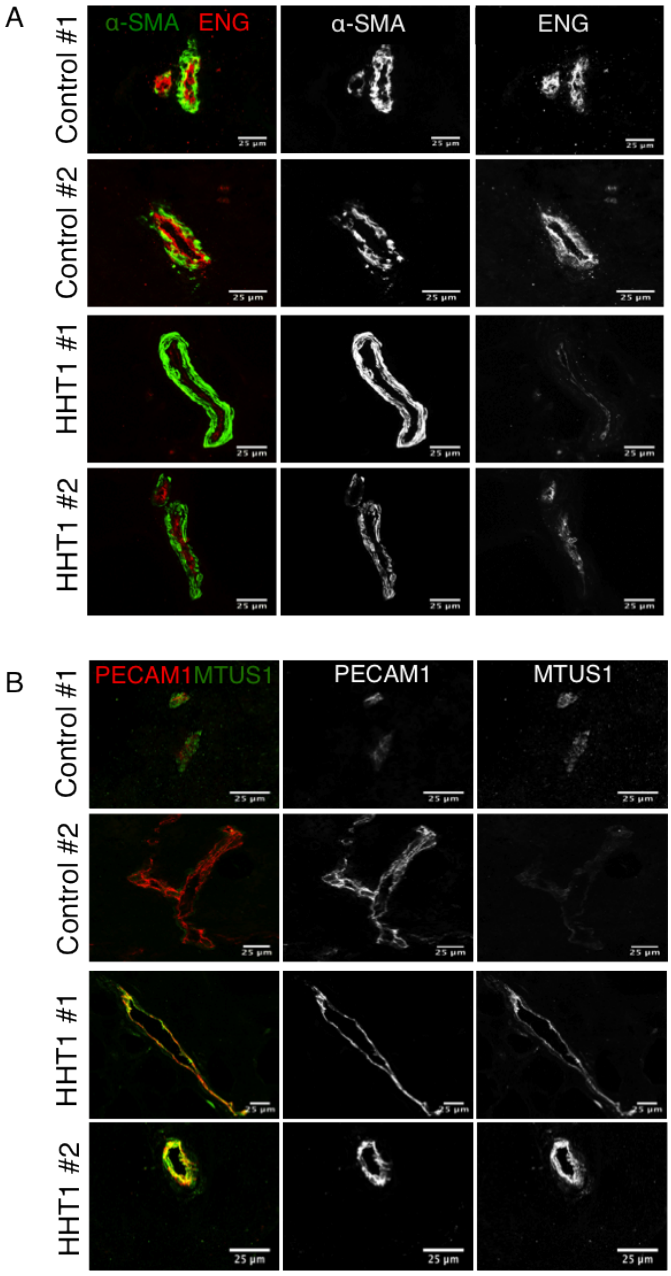

Supplementary Figure 4. HHT1 human skin exhibits increased MTUS1 protein levels. Additional confocal images of skin biopsies from Control and HHT1 subjects. A. α-SMA(green) and ENG (red) immunostaining. B. PECAM1 (red) and MTUS1 (green) immunostaining.

References:

Blanco, F.J., Santibanez, J.F., Guerrero-Esteo, M., Langa, C., Vary, C.P.H., and Bernabeu, C. (2005). Interaction and functional interplay between endoglin and ALK-1, two components of the endothelial transforming growth factor-β receptor complex. J. Cell. Physiol. *204*, 574–584.

Brown, M.A., zhao, Q., baker, K.A., naik, C., chen, C., pukac, L., singh, M., tsareva, T., parice, Y., mahoney, A., et al. (2005). Crystal Structure of BMP-9 and Functional Interactions with Pro-region and Receptors. Journal of Biological Chemistry *280*, 25111–25118.

Bundschu, K., and Schuh, K. (2014). Cardiovascular ATIP (Angiotensin receptor type 2 interacting protein) expression in mouse development. Developmental Dynamics *243*, 699–711.

Chan, N.L.M., Bourdeau, A., Vera, S., Abdalla, S., Gross, M., Wong, J., Cymerman, U., Paterson, A.D., Mullen, B., and Letarte, M. (2004). Umbilical Vein and Placental Vessels from Newborns with Hereditary Haemorrhagic Telangiectasia Type 1 Genotype are Normal despite Reduced Expression of Endoglin. Placenta *25*, 208–217.

Cheung, C., Bernardo, A.S., Trotter, M.W.B., Pedersen, R.A., and Sinha, S. (2012). Generation of human vascular smooth muscle subtypes provides insight into embryological origin–dependent disease susceptibility. Nat Biotechnol *30*, 165–175.

Choi, K.-D., Yu, J., Smuga-Otto, K., Salvagiotto, G., Rehrauer, W., Vodyanik, M., Thomson, J., and Slukvin, I. (2009). Hematopoietic and Endothelial Differentiation of Human Induced Pluripotent Stem Cells. Stem Cells *27*, 559–567.

Dambrot, C., van de Pas, S., van Zijl, L., ndl, B.B.X., Wang, J.W., Schalij, M.J., Hoeben, R.C., Atsma, D.E., Mikkers, H.M., Mummery, C.L., et al. (2013). Polycistronic lentivirus induced pluripotent stem cells from skin biopsies after long term storage, blood outgrowth endothelial cells and cells from milk teeth. Differentiation *85*, 101–109.

David, L., Mallet, C., Mazerbourg, S., Feige, J.J., and Bailly, S. (2007). Identification of BMP9 and BMP10 as functional activators of the orphan activin receptor-like kinase 1 (ALK1) in endothelial cells. Blood *109*, 1953–1961.

Di Benedetto, M., Bièche, I., Deshayes, F., Vacher, S., Nouet, S., Collura, V., Seitz, I., Louis, S., Pineau, P., Amsellem-Ouazana, D., et al. (2006). Structural organization and expression of human MTUS1, a candidate 8p22 tumor suppressor gene encoding a family of angiotensin II AT2 receptor-interacting proteins, ATIP. Gene *380*, 127–136.

Freund, C., Davis, R.P., Gkatzis, K., Ward-van Oostwaard, D., and Mummery, C.L. (2009). The first reported generation of human induced pluripotent stem cells (iPS cells) and iPS cell- derived cardiomyocytes in the Netherlands. Netherlands Heart Journal *18*, 51–54.

Freund, C., Davis, R.P., Gkatzis, K., Ward-van Oostwaard, D., and Mummery, C.L. (2010). The first reported generation of human induced pluripotent stem cells (iPS cells) and iPS cell-derived cardiomyocytes in the Netherlands. Netherlands Heart Journal *18*, 51–54.

Gougos, A., and Letarte, M. (1990). Primary Structure of Endoglin, an RGD-containing Glycoprotein of Human Endothelial Cells. The Journal of Biological Chemistry *265*, 8361–8364.

Goumans, M.-J., valdimarsdottir, G., Itoh, S., Lebrin, F., Larsson, J., Mummery, C., karlsson, S., and Dijke, ten, P. (2003). Activin Receptor-like Kinase (ALK)1 Is an Antagonistic Mediatorof Lateral TGF. Molecular Cell *12*, 817–828.

Kinnear, C., Chang, W.Y., Khattak, S., Hinek, A., Thompson, T., de Carvalho Rodrigues, D., Kennedy, K.,

Mahmut, N., Pasceri, P., Stanford, W.L., et al. (2013). Modeling and Rescue of the Vascular Phenotype of Williams-Beuren Syndrome in Patient Induced Pluripotent Stem Cells. Stem Cells Translational Medicine *2*, 2–15.

Kosla, J., Dvorak, M., and Cermak, V. (2013). Molecular analysis of the TGF-beta controlled gene expression program in chicken embryo dermal myofibroblasts. Gene *513*, 90–100.

Lebrin, F., Goumans, M.-J., jonker, L., Carvalho, R.L.C., valdimarsdottir, G., thorikay, M., Mummery, C., Arthur, H.M., and Dijke, ten, P. (2004). Endoglin promotes endothelial cell proliferation and TGF-b/ALK1 signal transduction. THE EMBO Journal *23*, 4018–4028.

Lebrin, F., Srun, S., Raymond, K., Martin, S., van den Brink, S., Freitas, C., ant, C.B.E., Mathivet, T., e, B.L.E., Thomas, J.-L.E.O., et al. (2010). Thalidomide stimulates vessel maturation and reduces epistaxis in individuals with hereditary hemorrhagic telangiectasia. Nat Med *16*, 420–428.

Nolan-Stevaux, O., Zhong, W., Culp, S., Shaffer, K., Hoover, J., Wickramasinghe, D., and Ruefli-Brasse, A. (2012). Endoglin Requirement for BMP9 Signaling in Endothelial Cells Reveals New Mechanism of Action for Selective Anti-Endoglin Antibodies. PLoS ONE *7*, e50920.

Orlova, V.V., Drabsch, Y., Freund, C., Petrus-Reurer, S., van den Hil, F.E., Muenthaisong, S., Dijke, P.T., and Mummery, C.L. (2013). Functionality of Endothelial Cells and Pericytes From Human Pluripotent Stem Cells Demonstrated in Cultured Vascular Plexus and Zebrafish Xenografts. Arteriosclerosis, Thrombosis, and Vascular Biology *34*, 177–186.

Orlova, V.V., van den Hil, F.E., Petrus-Reurer, S., Drabsch, Y., Dijke, ten, P., and Mummery, C.L. (2014). Generation, expansion and functional analysis of endothelial cells and pericytes derived from human pluripotent stem cells. Nat Protoc *9*, 1514–1531.

Ota, T., Fujii, M., Sugizaki, T., Ishii, M., Miyazawa, K., Aburatani, H., and Miyazono, K. (2002). Targets of transcriptional regulation by two distinct type I receptors for transforming growth factor-? in human umbilical vein endothelial cells. J. Cell. Physiol. *193*, 299–318.

Pardali, E., Goumans, M.-J., and Dijke, ten, P. (2010). Signaling by members of the TGF-Î² family in vascular morphogenesis and disease. Trends in Cell Biology *20*, 556–567.

pece-Barbara, N., Vera, S., Kathirkamathamby, K., Liebner, S., Di Guglielmo, G.M., Dejana, E., Wrana, J.L., and Letarte, M. (2005). Endoglin Null Endothelial Cells Proliferate Faster and Are More Responsive to Transforming Growth Factor 1 with Higher Affinity Receptors and an Activated Alk1 Pathway. Journal of Biological Chemistry *280*, 27800–27808.

Pece-Barbara, N., Cymerman, U., Vera, S., Marchuk, D.A., and Letarte, M. (1999). Expression analysis of four endoglin missense mutations suggests that haploinsufficiency is the predominant mechanism for hereditary hemorrhagic telangiectasia type 1. Human Molecular Genetics *8*, 2171–2181.

Petridou, S., Olga, M., spanakis, S., and Kazabn Masur, S. (2000). TGF-β Receptor Expression and Smad2 Localization Are Cell Density Dependent in Fibroblasts. Investigative Ophthalmology & Visual Science *41*, 89–95.

Rafii, S., Kloss, C.C., Butler, J.M., Ginsberg, M., Gars, E., Lis, R., Zhan, Q., Josipovic, P., Ding, B.S., Xiang, J., et al. (2013). Human ESC-derived hemogenic endothelial cells undergo distinct waves of endothelial to hematopoietic transition. Blood *121*, 770–780.

Shovlin, C.L. (2010). Hereditary haemorrhagic telangiectasia: Pathophysiology, diagnosis and treatment. Yblre *24*, 203–219.

Suzuki, Y., Ohga, N., Morishita, Y., Hida, K., miyazono, K., and Watabe, T. (2010). BMP-9 induces proliferation

of multiple types of endothelial cells in vitro and in vivo. Journal of Cell Science *123*, 1684–1692.

Takahashi, K., Tanabe, K., Ohnuki, M., Narita, M., Ichisaka, T., Tomoda, K., and Yamanaka, S. (2007). Induction of pluripotent stem cells from adult human fibroblasts by defined factors. Cell *131*, 861–872.

Thomas, B., Eyries, M., Montagne, K., Martin, S., Agrapart, M., Simerman-Francois, R., Letarte, M., and Soubrier, F. (2007). Altered endothelial gene expression associated with hereditary haemorrhagic telangiectasia. European Journal of Clinical Investigation 580–588.

Upton, P.D., Davies, R.J., Trembath, R.C., and Morrell, N.W. (2009). Bone Morphogenetic Protein (BMP) and Activin Type II Receptors Balance BMP9 Signals Mediated by Activin Receptor-like Kinase-1 in Human Pulmonary Artery Endothelial Cells. Journal of Biological Chemistry *284*, 15794–15804.

van Laake, L.W., van den Driesche, S., Post, S., Feijen, A., Jansen, M.A., Driessens, M.H., Mager, J.J., Snijder, R.J., Westermann, C.J.J., Doevendans, P.A., et al. (2006). Endoglin Has a Crucial Role in Blood Cell-Mediated Vascular Repair. Circulation *114*, 2288–2297.

Varelas, X., Samavarchi-Tehrani, P., Narimatsu, M., Weiss, A., Cockburn, K., Larsen, B.G., Rossant, J., and Wrana, J.L. (2010). The Crumbs Complex Couples Cell Density Sensing to Hippo-Dependent Control of the TGF-β-SMAD Pathway. Developmental Cell *19*, 831–844.

Witty, A.D., Mihic, A., Tam, R.Y., Fisher, S.A., Mikryukov, A., Shoichet, M.S., Li, R.-K., Kattman, S.J., and Keller, G. (2014). Generation of the epicardial lineage from human pluripotent stem cells. Nat Biotechnol 1–12.

Yu, J., Vodyanik, M.A., Smuga-Otto, K., Antosiewicz-Bourget, J., Frane, J.L., Tian, S., Nie, J., Jonsdottir, G.A., Ruotti, V., Stewart, R., et al. (2007). Induced pluripotent stem cell lines derived from human somatic cells. Science *318*, 1917–1920.

Zhang, J., Wilson, G.F., Soerens, A.G., Koonce, C.H., Yu, J., Palecek, S.P., Thomson, J.A., and Kamp, T.J. (2009). Functional Cardiomyocytes Derived From Human Induced Pluripotent Stem Cells. Circulation Research *104*, e30–e41.

Zieba, A., Pardali, K., Soderberg, O., Lindbom, L., Nystrom, E., Moustakas, A., heldin, C.H., and Landegren, U. (2012). Intercellular Variation in Signaling through the TGF- Pathway and Its Relation to Cell Density and Cell Cycle Phase. Molecular & Cellular Proteomics *11*, M111.013482–M111.013482.